Photoelectrochemical Characterization of Thin Films of Perylenetetracarboxylic Acid Derivatives

G. Tamizhmani and J. P. Dodelet*

INRS-Energie, C.P. 1020, Varennes, Québec, Canada J3X 1S2

R. Côté

Chemistry Department, Concordia University, Montréal, Québec, Canada H3G 1M8

D. Gravel

Département de chimie, Université de Montréal, Montréal, Québec, Canada H3C 3J7

Received April 24, 1991. Revised Manuscript Received September 3, 1991

Thin films of six N,N'-disubstituted diimide and a bisarylimidazole derivatives of 3,4,9,10-perylenetetracarboxylic acid have been sublimed on SnO_2 conductive substrates. Films grown at the substrate temperature of 160 ± 20 °C and at the rate of 0.8 ± 0.2 Å s^{-1} display essentially two morphologies: (i) long interwoven crystallites with their long axes being nearly parallel to the substrate surface and (ii) a more compact structure with, in some cases, the evidence of tight-packed crystallites growing in the direction perpendicular to the substrate surface. All perylene derivatives show a dominant photoanodic behavior. The photoactive interface is always between the perylene and the redox electrolyte (hydroquinone/benzoquinone). The nonporous or porous character of the films has been established electrochemically. The results of this study have been used for the interpretation of the presence or absence of a filtering effect in the action spectra and the differences in the quantum yield for electron collection with the direction of film illumination (front side vs back side).

Introduction

Besides their use as pigments in the dye and paint industries, derivatives of 3,4,9,10-perylenetetracarboxylic acid also display various interesting electrical properties. They are used as charge-generating materials, independently or along with other photoconductive pigments, in electrophotographic photoreceptors.[1-3] It has been shown that upon irradiation, both extrinsic (impurity controlled) and intrinsic charge-carrier generation originates from the first excited singlet state.[4] Perylene derivatives have also been used in heterojunctions with phthalocyanines in all organic photovoltaic[5-7] and photoelectrochemical cells.[8] Most of these reports suggest that perylene derivatives generally behave like n-type semiconductors.

Anodic photocurrents are also observed in photoelectrochemical cells with perylenetetracarboxylic dianhydride (PTCDA).[9] This pigment, which has been extensively used to produce contact barrier diodes with inorganic semiconductors,[10] is reported to be a p-type molecular semiconductor with a low charge carrier density.[11] The anodic photocurrents measured in electrochemical cells with PTCDA have been rationalized in terms of a preferential rate of hole injection in the solution and/or an asymmetrical spacial distribution of electron traps in the film with a larger concentration at the photoactive interface.[8,9]

The intent of the present work is to photoelectrochemically characterize a series of perylene derivatives in order to find (i) if all derivatives behave like photoanodes, (ii) which molecular structure is the most photoactive, and (iii) what are the roles of morphology and porosity of the perylene films. This information will allow us to pick the

Table I. Molecular Structures of Perylene Derivatives

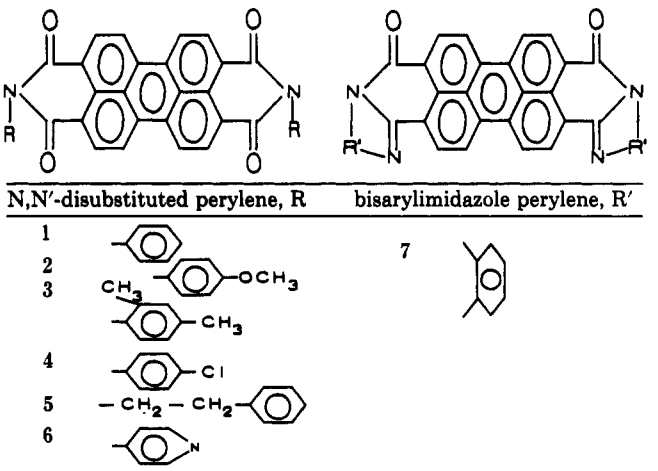

(1) (a) Loutfy, R. O.; Hor, A. M.; Hsiao, C. K.; Baranyi, G.; Kazmaier, P. *Pure Appl. Chem.* **1988**, *60*, 1047. (b) Hor, A. M.; Loutfy, R. O. U.S. Patent 4,587,189, 1986. (c) Nguyen, K. C.; Weiss, D. S. *Denshi Shashin Gakkaishi* **1988**, *27*, 2.

(2) Borsenberger, P. M.; Regan, M. T.; Staudenmayer, W. J. U.S. Patent 4,578,334, 1986.

(3) Loutfy, R. O.; Hor, A. M.; Kazmaier, P.; Tam, M. *J. Imag. Sci.* **1989**, *33*, 151.

(4) (a) Popovic, Z. D.; Loutfy, R. O.; Hor, A. M. *Can. J. Chem.* **1985**, *63*, 134. (b) Popovic, Z. D.; Hor, A. M.; Loutfy, R. O. *Chem. Phys.* **1988**, *127*, 451.

(5) Tang, C. W. *Appl. Phys. Lett.* **1986**, *48*, 183.

(6) (a) Panayotatos, P.; Parikh, D.; Sauers, R.; Bird, G.; Piechowski, A.; Husain, S. *Solar Cells* **1986**, *18*, 71. (b) Panayotatos, P.; Bird, G.; Sauers, R.; Piechowski, A.; Husain, S. *Solar Cells* **1987**, *21*, 301.

(7) (a) Forrest, S. R.; Leu, L. Y.; So, F. F.; Yoon, W. Y. *J. Appl. Phys.* **1989**, *66*, 5908. (b) Hiramato, M.; Kishigami, Y.; Yokoyama, M. *Chem. Lett.* **1990**, 119. (c) Hiramato, M.; Suezaki, M.; Yokoyama, M. *Chem. Lett.* **1990**, 327. (d) Morikawa, T.; Chikaya, A.; Tetsuo, T.; Shogo, S. *Nippon Kagaku Kaishi* **1990**, 962.

(8) Danziger, J.; Dodelet, J. P.; Lee, P.; Nebesny, K. W.; Armstrong, N. R. *Chem. Mater.* **1991**, *3*, 821.

(9) Danziger, J.; Dodelet, J. P.; Armstrong, N. R. *Chem. Mater.* **1991**, *3*, 812.

(10) (a) Forrest, S. R.; Kaplan, M. L.; Schmidt, P. H.; Feldmann, W. L.; Yanowski, E. *Appl. Phys. Lett.* **1982**, *41*, 90. (b) Forrest, S. R.; Kaplan, M. L.; Schmidt, P. H. *J. Appl. Phys.* **1984**, *55*, 1492. (c) Forrest, S. R.; Kaplan, M. L.; Schmidt, P. H. *J. Appl. Phys.* **1984**, *56*, 543. (d) Forrest, S. R.; Kaplan, M. L.; Schmidt, P. H. *Annu. Rev. Mater. Sci.* **1987**, *17*, 189. (e) So, F. F.; Forrest, S. R. *J. Appl. Phys.* **1988**, *63*, 442.

(11) Forrest, S. R.; Kaplan, M. L.; Schmidt, P. H. *J. Appl. Phys.* **1984**, *55*, 1492.

0897-4756/91/2803-1046$02.50/0

Table II. Physical Properties of Perylene Derivatives

material	sublimation temp, °C	film color	film abs max: major, minor, nm	film abs coeff for major peak, cm^{-1}
1	390	red	460, 570, 540	1.6×10^4
2	390	red	480, 560	4.8×10^4
3	390	red	490, 535, 460	2.9×10^4
4	390	red	450, 540, 560	2.0×10^4
5	390	blue	460, 620	3.2×10^4
6	420	red	480, 560	4.9×10^4
7	450	blue	540, 670	5.0×10^4

best candidate to build a heterojunction with chloroaluminum phthalocyanine, a highly photoactive p-type semiconductor that we have already extensively characterized.[12,15]

The various perylene derivatives synthesized for this work were chosen for the following reasons: the phenyl-, methoxyphenyl-, dimethylphenyl-, and chlorophenylbenzimide derivatives would test an eventual influence of electron-donating or -withdrawing groups; the pyridinylbenzimide derivative would check the influence of a reaction of the material with one of the redox electrolytes. Some properties (film morphology,[13,14] crystallinity,[2] photoactivity as carrier generator[2,3]), are already known for the two remaining compounds, viz., the phenylethylbenzimide and the arylimidazol derivatives. Those reports help in the interpretation of the results obtained in this work.

Experimental Section

Synthesis and Purification of Materials. A series of six N,N'-disubstituted 3,4,9,10-perylenetetracarboxylic acid diimide and one bisarylimidazole 3,4,9,10-perylenetetracarboxylic acid were synthesized. The chemical structures of these pigments (1–7) are given in Table I. All chemicals (highest purity available from Aldrich) were used without further purification for the preparation of perylene derivatives. In the synthesis procedures described in the literature[16] a cosolvent is often used. When it was possible, this was avoided in the present work in order to reduce the amount of impurities susceptible to alter the electrical properties of the organic films. A detailed experimental procedure is given for the synthesis of each compound.

All these materials were purified a minimum of two times in a tubular furnace under vacuum (ca. 10^{-6} Torr) at the temperatures specified in Table II. The temperatures mentioned in Table II were the temperatures at which the source materials start to sublime. Compound 7 could exist in both cis and trans forms. The nearly similar volatilities for both forms do not allow their separation by sublimation.[3] The necessary number of sublimations was established by testing the films of each sublimed product of compounds 5 and 7 for photoelectrochemical response in hydroquinone/potassium hydrogen phthalate (0.2 M/0.2 M) at pH 3.9. A second sublimation improved the photocurrent from the first sublimation by nearly 1 order of magnitude. The third and fourth sublimations did not improve the photocurrent further. It was assumed that the other compounds would also behave similarly.

Infrared (IR) spectra were recorded on a Bowen Michelson 102 Fourier transform spectrometer using KBr disks. The intensity of the bands is described as weak (w), strong (s) or broad (br).

Elemental analyses have been performed on all the pigments by Galbraith Laboratories Inc., Knoxville, TN, on products purified by sublimation.

2,9-Diphenylanthra[2,1,9-*def*:6,5,10-*d'e'f'*]diisoquinoline-1,3,8,10(2*H*,9*H*)-tetrone (1). The typical procedure followed for the preparation of all perylene derivatives is discussed as follows: 3,4,9,10-perylenetetracarboxylic dianhydride (5.0 g, 12.7 mmol) suspended in aniline (50 g, 0.54 mol) was heated at 184 °C for 4 days under nitrogen. The pigment was then of a uniform violet color. The suspension was suction filtered (using sintered glass), and the solid residue was washed with 150 mL of hot benzene followed by 100 mL of acetonitrile. The resulting dark red fine crystals were dried under vacuum, yield 6.65 g (96% of theoretical value); IR (cm^{-1}) 3050 (CH, w), 1702 and 1660 (C=O, s), 1590, 1353 (s), 1254. The IR spectrum of the crude reaction product was identical to the IR spectrum of the material purified by sublimation. The starting product, perylenetetracarboxylic dianhydride (strong characteristic broad band at 1759 cm^{-1}, ν(C=O)), could not be detected in any of the IR spectra. Anal. Calcd for $C_{36}H_{18}N_2O_4$: C, 79.69; H, 3.34; N, 5.16. Found: C, 79.28; H, 3.34; N, 5.08.

2,9-Bis(4-methoxyphenyl)anthra[2,1,9-*def*:6,5,10-*d'e'f'*]diisoquinoline-1,3,8,10(2*H*,9*H*)-tetrone (2). 3,4,9,10-Perylenetetracarboxylic dianhydride (5.73 g, 14.6 mmole) suspended in *p*-anisidine (60.1 g, 0.488 mol) was heated at 240 °C for 2 days under nitrogen. The washed and dried product was recovered as fine brown needles, yield 97% (8.52 g); IR (cm^{-1}) 3070, 2938 and 2826 (CH, w), 1698 and 1664 (C=O, s), 1589, 1509, 1350 (s), 1251 (s), 1033. Anal. Calcd for $C_{38}H_{22}N_2O_6$: C, 75.74; H, 3.68; N, 4.65. Found: C, 74.76; H, 3.70; N, 4.58.

2,9-Bis(2,4-dimethylphenyl)anthra[2,1,9-*def*:6,5,10-*d'e'f'*]diisoquinoline-1,3,8,10(2*H*,9*H*)-tetrone (3). 3,4,9,10-Perylenetetracarboxylic dianhydride (3.0 g, 7.65 mmol) suspended in 2,4-dimethylaniline (20 g, 0.165 mol) was heated at 218 °C for 4 days under nitrogen. The washed and dried product was recovered as dark orange needles with a yield of 91% (4.20 g); IR (cm^{-1}) 3077, 3022 and 2967 (CH, w), 1705 and 1662 (C=O, s), 1586, 1349 (s), 1251, 1182, 804 (br). Anal. Calcd for $C_{40}H_{26}N_2O_4$: C, 80.25; H, 4.38; N, 4.68. Found: C, 79.75; H, 4.50; N, 4.49.

2,9-Bis(4-chlorophenyl)anthra[2,1,9-*def*:6,5,10-*d'e'f'*]diisoquinoline-1,3,8,10(2*H*,9*H*)-tetrone (4). 3,4,9,10-Perylenetetracarboxylic dianhydride (3.0 g, 7.65 mmol) suspended in 4-chloroaniline (25.0 g, 0.196 mol) was heated at 230 °C for 1 day under nitrogen. The washed and dried product was contaminated by decomposition products arising from 4-chloroaniline; IR (cm^{-1}) 3078 (CH, w), 1701 and 1667 (C=O, s), 1588, 1347 (s), 1252, 1087, 831. Anal. Calcd for $C_{36}H_{16}Cl_2N_2O_4$: C, 70.71; H, 2.64; Cl, 11.60; N, 4.58. Found: C, 71.04; H, 2.77; Cl, 11.42; N, 4.47.

2,9-Bis(2-phenylethyl)anthra[2,1,9-*def*:6,5,10-*d'e'f'*]diisoquinoline-1,3,8,10(2*H*,9*H*)-tetrone (5). 3,4,9,10-Perylenetetracarboxylic dianhydride (5.05 g, 12.9 mmol) suspended in phenethylamine (50 g, 0.413 mol) was heated at 200 °C for 2 days under nitrogen. The washed and dried product was recovered as a dark green powder contaminated by insoluble organic impurities (8.09 g of crude product); IR (cm^{-1}) 3022 and 2950 (CH, w), 1692 and 1653 (C=O, s), 1583, 1342 (br), 1260, 1012, 443. Anal. Calcd for $C_{40}H_{28}N_2O_4$: C, 80.25; H, 4.38, N, 4.68. Found: C, 77.63; H, 4.24; N, 4.52.

2,9-Bis(4-pyridyl)anthra[2,1,9-*def*:6,5,10-*d'e'f'*]diisoquinoline-1,3,8,10(2*H*,9*H*)-tetrone (6). 3,4,9,10-Perylenetetracarboxylic dianhydride (3.11 g, 7.93 mmol) suspended in 4-aminopyridine (10 g, 0.106 mol) and dimethylnaphthalene (50 mL) was refluxed for 1 day under nitrogen. The washed and dried product was recovered as red-orange fine crystals, yield 3.94 g (91% of theoretical value); IR (cm^{-1}) 3059 (CH, w), 1700 and 1666 (C=O, s), 1582, 1347 (s), 1255, 789, 533. Anal. Calcd for $C_{34}H_{16}N_4O_4$: C, 74.99; H, 2.96; N, 10.29. Found: C, 74.44; H, 3.04; N, 9.50.

Bisbenzimidazo[2,1-*a*:1',2'-*b*']anthra[2,1,9-*def*:6,5,10-*d'e'f'*]diisoquinoline-6,11-dione (7, Cis Isomer) and Bis-

(12) (a) Guay, D.; Veilleux, G.; Saint-Jacques, R. G.; Côté, R.; Dodelet, J. P. *J. Mater. Res.* **1989**, *4*, 651. (b) Tourillon, G.; Côté, R.; Guay, D.; Dodelet, J. P. *J. Electrochem. Soc.* **1989**, *136*, 2931. (c) Guay, D.; Tourillon, G.; Gastonguay, L.; Dodelet, J. P.; Nebesny, K. W.; Armstrong, N. R. *J. Phys. Chem.* **1991**, *95*, 251. (d) Dodelet, J. P.; Gastonguay, L.; Veilleux, G.; Saint-Jacques, R. G.; Côté, R.; Guay, D.; Tourillon, G. Photochemistry and photoelectrochemistry of organic and inorganic molecular thin films. *Proc. SPIE* **1991**, *1436*, 38.

(13) Kam, K. K.; Debe, M. K.; Poirier, R. J.; Drube, A. R. *J. Vac. Sci. Technol.* **1987**, *A5*, 1914.

(14) Debe, M. K.; Kam, K. K.; Liu, J. C.; Poirier, R. J. *J. Vac. Sci. Technol.* **1988**, *A6*, 1907.

(15) Guay, D.; Dodelet, J. P.; Côté, R.; Langford, C. H.; Gravel, D. *J. Electrochem. Soc.* **1989**, *136*, 2272.

(16) (a) Maki, T.; Hashimoto, H. *Bull. Chem. Soc. Jpn.* **1952**, *25*, 411; **1954**, *27*, 602. (b) Rademacher, A.; Märkle, S.; Langhals, H. *Chem. Ber.* **1982**, *115*, 2927.

benzimidazo[2,1-*a*:2',1'-*a'*]anthra[2,1,9-*def*:6,5,10-*d'e'f'*]diisoquinoline-10,21-dione (7, Trans Isomer). 3,4,9,10-Perylenetetracarboxylic dianhydride (2.01 g, 5.12 mmol) suspended in 1,2-phenylenediamine (20 g, 0.185 mol) and dimethylnaphthalene (50 mL) was refluxed for 1 day under nitrogen. The washed and dried reaction product was recovered as olive-green fine crystals, yield 2.67 g (97% of theoretical value); IR (cm^{-1}) 1685 (C=O, s), 1589, 1541, 1442, 1354 (s) 1234, 747 (s). Anal. Calcd for $C_{36}H_{16}N_4O_2$: C, 80.58; H, 3.00; N, 10.44. Found: C, 78.38, H, 2.82; N, 9.76.

Electrode Preparation and Measurements. The perylene films were obtained by sublimation under vacuum ($\sim 10^{-6}$ Torr) onto highly conducting SnO_2 substrates (ρ_s = 25–30 Ω sq^{-1}) precleaned with methanol and sulfochromic acid soaking for 30 min. The sublimation rate was around 0.6–1 Å/s. All the materials were sublimed at substrate temperatures of 160 ± 20 °C. Compound **5** was also sublimed over conducting SnO_2 substrates maintained at room temperature by circulating water over the base of the substrate.

The thickness of few thick films of all the materials was measured using a Sloan Dektak 3030 profilometer. The absorption coefficient of the major peak of each pigment was deduced from a plot of the absorbance maximum versus the measured film thickness. The absorption coefficient value thus obtained was used to calculate the thickness of very thin films.

For scanning electron microscopy (SEM) studies, a Hitachi S570 instrument was used. A thin gold layer was deposited over the films to avoid the surface charging.

The electrochemical and photoelectrochemical experiments were carried out in a conventional three-electrode, one-compartment cell. A platinum foil served as the counter electrode, and a saturated calomel electrode (SCE) as the reference electrode. The films with an epoxy-defined active area of 2.3 cm^2 were used as working electrodes. A slowly modulated white light from a 450-W Xe arc lamp with a 10-cm water filter and a 385-nm cuton UV filter was used for photoelectrochemical measurements. The white light intensity at the level of the working electrode (usually 35 mW cm^{-2}) was measured with a Scientech 362 power energy meter. Neutral density filters were used to obtain lower light intensities. Monochromatic light used in action spectra measurements was obtained from the forementioned lamp and 10-nm-bandwidth interference filters of different wavelength. The monochromatic light was focused onto the cell, and its intensity was measured with a Coherent (Model 212) power meter. Current–voltage measurements were performed with a PAR Model 173 potentiostat and a PAR Model 175 voltage programmer. Voltametric data were obtained at a scan rate of 5 mV/s in hydroquinone (H_2Q)/potassium hydrogen phthalate (KHP) solutions and of 100 mV/s in Fe $(CN)_6^{3-/4-}$ electrolyte. Action spectra measurements were carried out for both front-side and back-side illuminations at 0.3 V vs SCE in H_2Q/KHP electrolyte. We define the illumination of electrolyte/perylene interface first and SnO_2/perylene interface first, respectively, as front-side (FS) and back-side (BS) illuminations. All the chemicals necessary for this work were research grade and they were used without purification. All electrochemical experiments were carried out in high-purity argon-bubbled solutions.

Results and Discussion

Scanning Electron Microscopy (SEM). SEM studies of all the pigments were carried out on relatively thick films (>2600 Å) in order to avoid the influence of surface morphology of the substrates. The morphology of the SnO_2 substrate has already been depicted.[15]

Figure 1 presents micrographs of compounds **1**, **4**, **5**, and **7** for the films used for photoelectrochemical studies. All these films are made of elongated crystallites (up to a few microns long) having their long axes in a direction roughly parallel to the substrate surface. An as-sublimed film of compound **4** was also observed by SEM. It displays essentially the same morphology as that of the film obtained after contact with the electrolyte.

Figure 2a–c presents micrographs of compounds **3**, **6**, and **2** at the same magnification. Figure 2d presents the micrograph of compound **2** at a higher magnification than Figure 2c. All the films of Figure 2 were used previously for photoelectrochemical studies. Films of materials **3** and **6** show flakelike tiny crystallites, while films of compound **2** display a rather compact structure similar to the morphology of a columnar growth. This is indeed more obvious in Figure 2d. Apart from some inhomogeneties in the organic film structure, the morphology of compound **2** is an exact replica of the morphology of the SnO_2 substrate. The crystallites of pigment **2** seem therefore to grow in a direction perpendicular to the substrate surface. Micrographs of the as-sublimed film of material **2** display essentially the same background as Figure 2c except for the tiny filaments lying flat on the surface. These filaments disappear after contact with the electrolyte.

It has already been mentioned[13,14] that the physical structure of organic films formed from the vapor phase ranges over a scale that is enormous compared to inorganic materials. The morphology of large heterocyclic molecular films depends drastically on growth rates and substrate temperatures. Studies have been performed by Debe et al.[14] on compound **5**. Films of that pigment were grown at rates betwen 3 and 30 Å s^{-1} and substrate temperatures ranging from −165 to 153 °C. The large morphology changes observed for those films were interpreted by the coexistence of two polymorphs. At a substrate temperature below 100 °C, the percentage of formation of one polymorph over the other would depend on the arrival rate of molecules from the gas phase. This would not be true anymore above 100 °C, where the surface mobility of the molecules would be adequate and the rates would not be anymore a significant factor in determining the type of microstructure observed.

Films of compound **5** grown at 153 °C by Debe et al. display the same morphology as that depicted in Figure 1c (and also Figure 1a,b,d for compounds **1**, **4**, and **7**) for the same compound grown in the present work at a substrate temperature of about 160 °C and a rate of about 0.8 Å s^{-1}. At lower substrate temperatures (below 100 °C) the morphology of films of compound **5** grown by Debe et al. at rates of about 3 Å s^{-1} shows similarities with those reported in Figure 2 for compounds **3**, **6**, and **2**, all grown at around 160 °C with the rates of about 0.8 Å s^{-1}. It is reasonable to suggest that based on the presence of different polymorphs the morphological behavior of compound **5** (and perylene red[13]) could also hold good for other perylene derivatives but with transition temperatures varying from one pigment to the other.

Electrochemistry and Photoelectrochemistry. (A) Current–Voltage Characteristics. Figure 3 presents the current–voltage curves of films of compounds **1** and **2** under slowly modulated white light illumination (35 mW cm^{-2}) in H_2Q/KHP (0.2 M/0.2 M) electrolyte, at pH 3.9. E_{redox} was measured at 0.175 V. Both curves were recorded from positive to negative applied voltages.

All pigments investigated in this work display both anodic and cathodic photocurrents. The amplitude of the anodic photocurrent varies from compound **1** to **7**. In general, there is a 10–15% decay in the initial photocurrent in the first 15 min for all the materials except **2**, to which no photocurrent decay is observed. Table III reports the stabilized photocurrent densities measured at 0.3 V. Except for compound **4**, all the other pigments are at least about 1 order of magnitude less photoactive than the methoxybenzene derivative.

All compounds show a similar cathodic photoactivity. Photocurrent densities under white light illumination never exceeds about 5 μA cm^{-2}. The larger cathodic

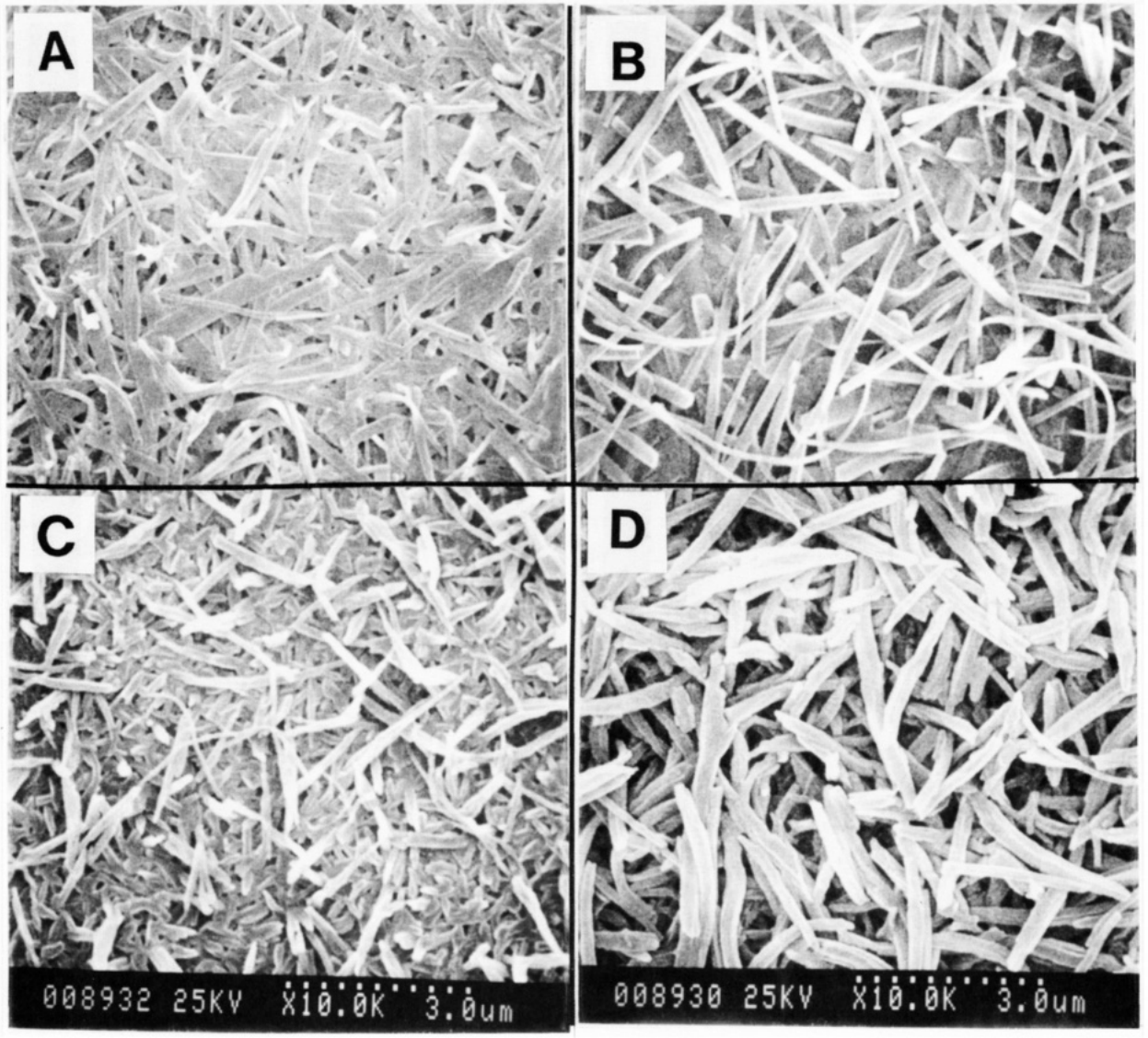

Figure 1. SEM micrographs of thin films of perylene derivatives: compounds **1** (A), **4** (B), **5** (C), and **7** (D).

Table III. Photoelectrochemical[a] Properties of Perylene Derivatives

material	photocurrent,[b] μA cm^{-2}	porous film	slope value of plot ln J vs ln I	max quantum yield for front side illum, %	max quantum yield for back side illum, %	film thickness, Å
1				0.7	0.7	620
	13 (5350)	yes	0.63	0.5	0.8	5350
				0.2	0.5	11440
2				1.5	0.4	1750
	217 (2600)	no	0.94	2.7	0.8	2600
				0.4	0.1	3270
3				0.8	1.3	1260
	35 (1260)	yes	0.89	0.5	0.8	2240
				0.4	0.1	4230
4				0.8	0.8	700
	59 (1550)	yes	0.81	1.2	1.4	1500
				0.9	1.3	4400
5				0.3	0.3	420
	15 (2680)	no	0.80	0.5	0.3	2680
				0.4	0.2	5410
6				0.2	0.3	130
	22 (1060)	yes	0.73	1.1	1.2	1060
				1.0	1.1	3460
7				0.4	0.3	960
	28 (3520)	yes	0.77	0.3	0.6	2400
				0.3	0.8	3520

[a] All photocurrent and quantum yield values are reported under 0.3 V applied to the film in contact with H_2Q/KHP (0.2 M/0.2 M) electrolyte. [b] White light (35 mW cm^{-2}); front side illumination; film thickness (Å) is given in parentheses.

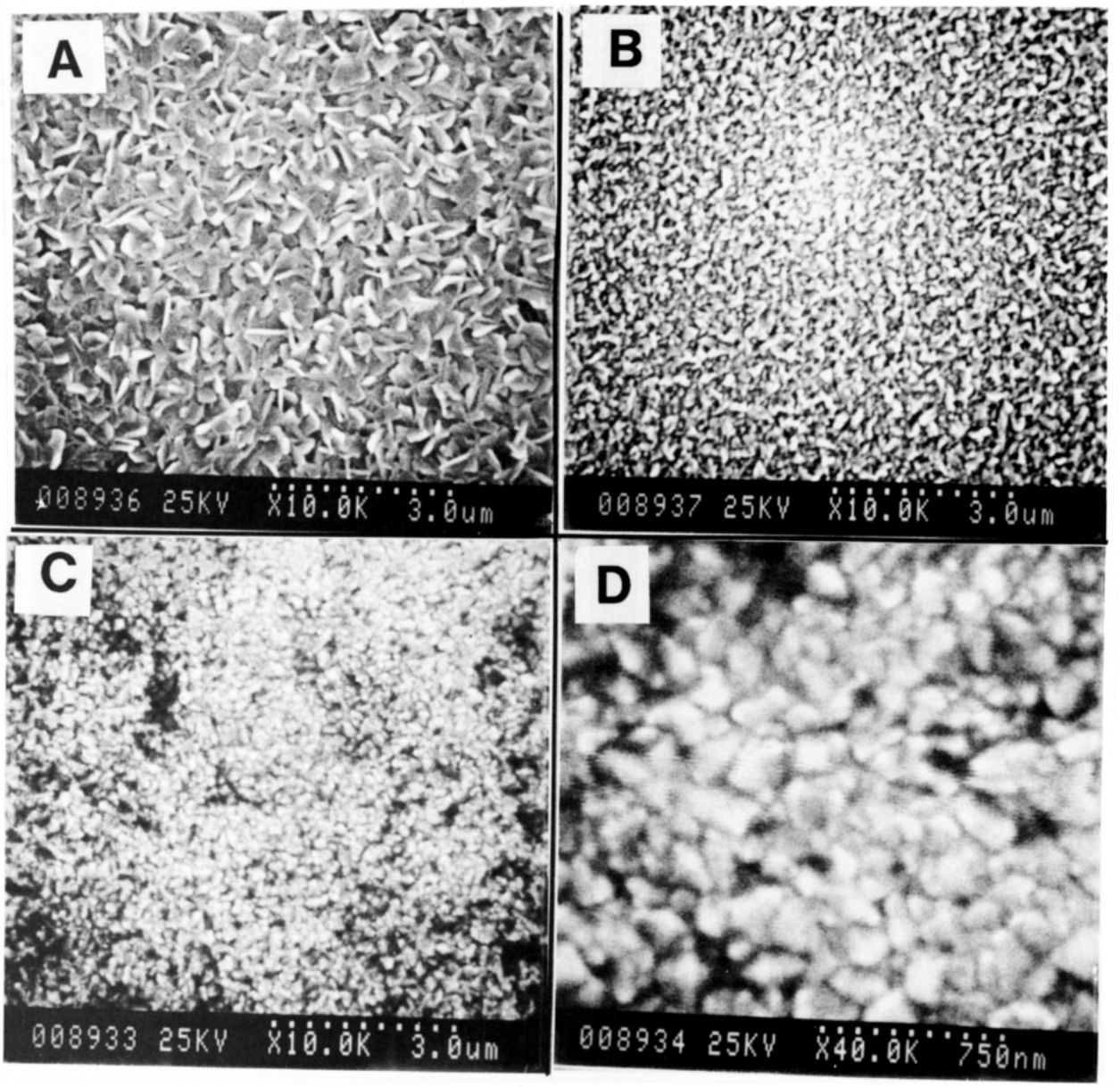

Figure 2. SEM micrographs of thin films of perylene derivatives: compounds **3** (A), **6** (B), **2** (C), under a magnification of 10^4, and **2** (D), under a magnification of 4×10^4.

transient photocurrents seen in Figure 3B are due to capacitive effects: charges are photogenerated then recombine within the film. The addition of benzoquinone (BQ = 0.002 M) to H_2Q/KHP electrolyte enhances the cathodic photocurrent only for compound **5**. At the same time, the anodic photocurrent of that pigment decreases by a factor of about 2. The cathodic photocurrent is now the dominant one. It increases with the applied voltage without reaching saturation in the potential range investigated. A cathodic photocurrent density of about 100 μA cm^{-2} has been measured at −0.6 V for compound **5**.

The coexistence of anodic and cathodic photocurrents, depending upon the applied potential, is characteristic of a rather insulating material whose conductivity varies with the absorption of light. For the most resistive films, a simplified parallelogram energy level diagram can be assumed for the organic phase. When a sufficient positive potential is applied and the electrode is illuminated, an anodic current is observed while a cathodic current is observed for a negative bias on the electrode.[16] In the present work, the potential at which the photocurrent changes its sign is about −0.050 V. This would likely correspond to the value of the flatband potential for the pigment.[17] The relative importance of both photocurrents is governed by the possibility of transferring the photogenerated charges across the interfaces.

All perylene films of this work are derivatives of the 3,4,9,10-perylenetetracarboxylic dianhydride (PTCDA). This material has been identified as a p-type molecular semiconductor with a very low charge carrier density (p = ca. 5×10^{14} cm^{-3}).[11] However, only anodic photocurrents were detected for that material.[9] The main photocurrents of PTCDA derivatives measured in this work are also anodic. Therefore, it does not mean that these pigments are necessarily n-type semiconductors.

Furthermore, the results of our studies are not in line with the effect toward increasing (or decreasing) the n-type character of perylene derivatives as proposed by Panayotatos et al.[6] by substitution with electron-withdrawing atoms such as Cl (or electron-donating groups such as

(17) (a) Jaeger, C. D.; Fan, F.-R.; Bard, A. J. *J. Am. Chem. Soc.* **1980**, *102*, 2592. (b) Gireaudeau, A.; Fan, F.-R.; Bard, A. J. **1980**, *102*, 5137. (c) Bélanger, D.; Dodelet, J. P.; Dao, L. H.; Lombos, B. A. *J. Phys. Chem.* **1984**, *88*, 4288.

(18) Tachikawa, H.; Faulkner, L. R. *J. Am. Chem. Soc.* **1978**, *100*, 4379.

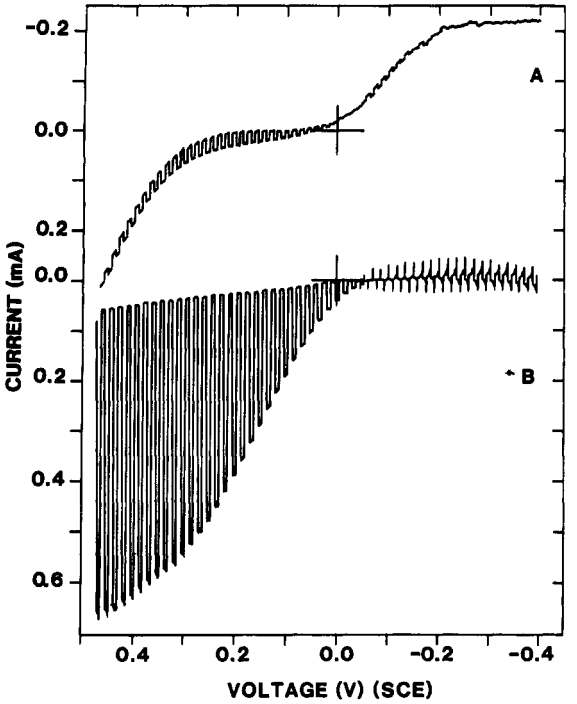

Figure 3. Current–voltage curves of films of compounds 1 (A) and 2 (B) under modulated white light at 35 mW cm^{-2} with H_2Q/KHP as electrolyte.

OCH_3). As can be seen in Table III, compound 4 is characterized by a lower anodic photocurrent density than compound 2. The reverse would have been expected for n-type semiconductors on the basis of the inductive properties of Cl atoms or methoxy and methyl groups. Molecular packing in the solid state probably plays a more prominent role for these large substituted heterocycles. Molecular packing is quite sensitive to substitution as it has been shown by X-ray diffraction studies.[19]

The n-type nature of organic semiconductors would probably be due to partially reduced molecular solids. They would be highly air-sensitive unless their electron affinities are higher than that of oxygen. It has been shown for phthalocyanines that the substitution on the macrocycle affects both HOMO and LUMO orbitals in the same way.[20] A large peripheral substitution of strongly electron-withdrawing groups has been proposed to lead to n-type organic semiconductors stable in air,[21] but this still remains to be demonstrated experimentally.

Curves A–D of Figure 4 respectively represent the dark current–voltage characteristics of compounds 1, 2, 5, and a bare SnO_2 electrode in $Fe(CN)_6^{3-/4-}$ electrolyte (2.5×10^{-3} M/2.5×10^{-3} M) at pH 6. $Fe(CN)_6^{3-/4-}$ is a quasi-reversible electrolyte on SnO_2.[22] Curve A demonstrates that the redox electrolyte still has the access to SnO_2 through the bulk of compound 1, and hence this material is porous. Curve A is also typical of compounds 3, 4, 6, and 7. On the contrary, curves B and C demonstrate that compounds 2 and 5 are nonporous. Curve C is typical of a highly resistive material, whereas the curve B of compound 2 displays some rectification. It indicates the presence of a space charge developed in the film in contact with the

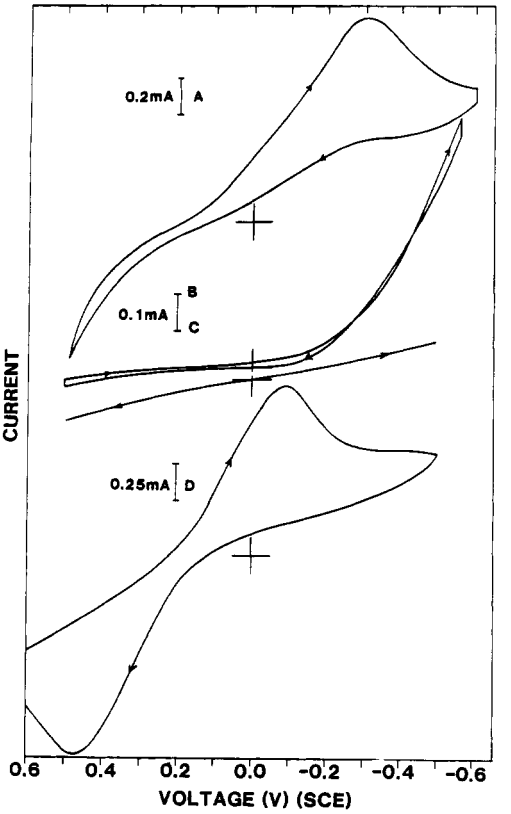

Figure 4. Current–voltage curves in the dark of compounds 1 (A), 2 (B), and 5 (C) and a bare SnO_2 electrode (D) with $Fe(CN)_6^{3-/4-}$ electrolyte.

redox electrolyte. It is to be noticed that it is not possible to assess the nonporous character of the films of compound 5 just on the basis of the SEM micrograph of their surface (Figure 1C).

The redox electrolyte H_2Q/BQ is quite irreversible on SnO_2.[22] Therefore, an important dark electrochemistry decreasing the photoeffect is not expected to occur in the voltage range explored in this work.

Besides H_2Q/BQ, I_3^-/I^- (5×10^{-3} M/5×10^{-2} M) was also used with compound 6 for which some reaction was expected between iodine and the lone electron pair of nitrogen in the substituted perylene. A very small (<5 μA cm^2) cathodic photocurrent was observed and found to be superimposed on the dark I–V curve showing poor rectification.

(B) Absorption and Action Spectra. There was no change in the absorption spectra of perylene derivatives due to repeated purification by sublimation. The absorption maxima in the visible region and the corresponding linear absorption coefficients are given in Table II. Typical absorption spectra are presented in Figures 5 and 6 for compounds 2 and 6, respectively. The maxima and shape of absorption spectra of varying thickness of all the materials, except material 7, were found to be the same. For material 7, there was a spreading of peaks by a few nanometers for thick films.

Absorption spectra (and therefore color) of perylene pigments in the solid state are not only determined by the electronic properties of the individual molecular chromophores but are also influenced by the electronic interactions with the vicinal molecules. In the crystal, longitudinal and/or lateral translations or even rotations occur between stacked perylene derivatives to avoid unfavorable interactions. Graser and Hädicke[23] found that the tran-

(19) Klebe, G.; Graser, F.; Hädicke, E.; Berndt, J. *Acta Crystallogr.* **1989**, *B45*, 69.

(20) (a) Wöhrle, D.; Schmidt, V. *J. Chem. Soc., Dalton Trans.* **1988**, 549. (b) Louati, A.; El Meray, M.; André, J. J.; Simon, J.; Kadish, K. M.; Gross, M.; Gireaudeau, A. *Inorg. Chem.* **1985**, *24*, 1175.

(21) Hale, P. D.; Pietro, W. J.; Ratner, M. A.; Ellis, D. E.; Marks, T. J. *J. Am. Chem. Soc.* **1987**, *109*, 5943.

(22) Bélanger, D.; Dodelet, J. P.; Lombos, B. A. *J. Electrochem. Soc.* **1986**, *133*, 1113.

(23) Graser, F.; Hädicke, E. *Liebigs. Ann. Chem.* **1984**, 483.

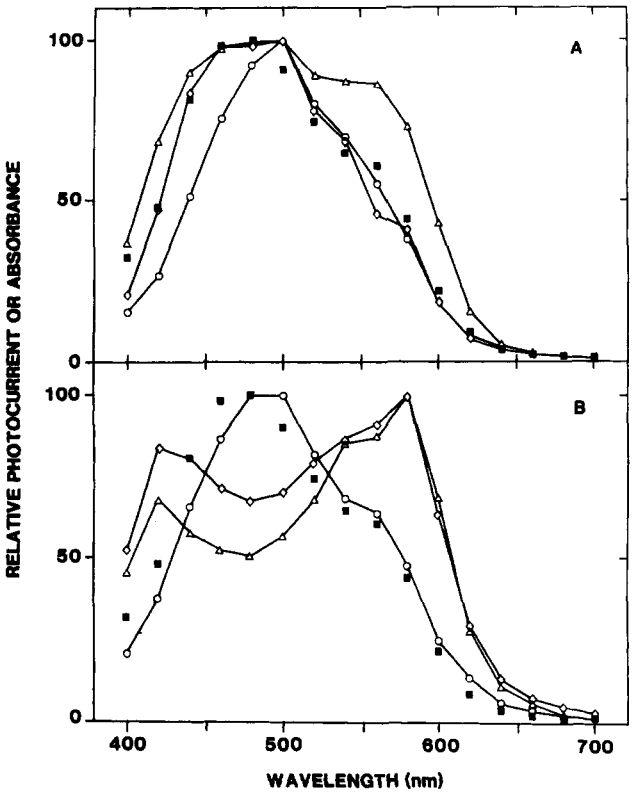

Figure 5. Absorption (■) and action spectra of compound **2** for front (A) and back (B) illuminations. Film thickness: 330 Å (○), 1750 Å (◇), 2600 Å (△).

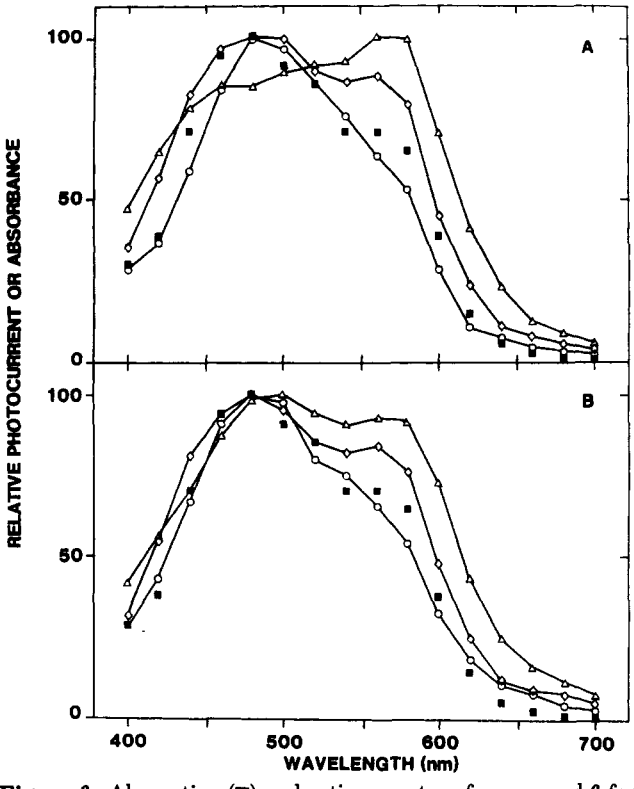

Figure 6. Absorption (■) and action spectra of compound **6** for front (A) and back (B) illuminations. Film thickness: 130 Å (○), 1060 (◇), 3460 Å (△).

sverse shift of neighboring molecules in the stack is a prominent factor for determining the differences in color of the pigments.

It is to be noted that there was no change in absorption spectra of all these materials after electrochemical and photoelectrochemical characterizations. It indicates therefore that these measurements did not alter the chemical nature or the structural characteristics of the films. On the other hand, it has already been reported that changes in the substrate temperature maintained during film sublimtion have a great influence on the absorption spectrum[2,14] and crystallinity[2] of compound **5** (and other perylene derivatives too[13]). An amorphous film is obtained when the substrate temperature is maintained at around room temperature. This material shows a reduced absorbance range centered around 500 nm compared to the broader absorption of the crystalline films with maxima at about 460 and 620 nm. The photoactivity of the amorphous compound **5** is also measured in this work to compare with the photoactivity of the crystalline compound **5** given in Table III. Under white light illumination, the anodic photocurrent density at 0.3 V of the amorphous film is about one-third of the corresponding crystalline value.

Figures 5 and 6 present the normalized action spectra for various thicknesses of compounds **2** and **6**, respectively. Each figure depicts two parts: A, front side illumination, and B, back side illumination. The action spectra are corrected for a constant photon flux using the following equation:

$$J = kI^{\gamma} \quad (1)$$

where J is the photocurrent density, k is proportionality constant, and I is the incident light intensity. In the present case, J is measured at 0.3 V in H_2Q/KHP electrolyte. The mean values of the exponent (γ) measured at 400, 500, and 600 nm are reported in Table III for the various materials. The individual values were found to be nearly constant, and the mean values were always between 0.6 and 1. The sublinear intensity dependence of the photocurrent is typical of a solid containing traps characterized by an exponential distribution in energy.[24]

Table III also reports the maximum quantum yields for front and back side illuminations at +0.3 V in H_2Q/KHP electrolyte. They correspond to the wavelength for which a value of 100% is obtained on the normalized action spectra. The quantum yield for current collection is given by the following relation:

$$\phi(\%) = \frac{\text{number of collected electrons}}{\text{number of incident photons}} \times 100 \quad (2)$$

It is surprising to note that the quantum yield value of individual films of all the materials except **2** and **5** is higher for back-side than for front-side illumination. This can be explained by the porous nature of the films of materials **1**, **3**, **4**, **6**, and **7** and the nonporous nature of the films of materials **2** and **5**. When the film is porous, the entire crystallite is in contact with the electrolyte except for regions where two crystallites meet (see Figure 1) or regions where a crystallite contacts the SnO_2 substrate. For an efficient collection of photogenerated charges, holes and electrons have to be quickly separated from each other before their recombination occurs. Holes resulting from the dissociation of excitons near the illuminated interface can be injected into the solution where they react with the reducing agent, from nearly the entire surface of the crystallite. On the other hand, the excess electrons in the film have to be removed through the SnO_2 substrate. This will be faster for an excess electron generated near the substrate than far away from it. If the drift mobility of

(24) (a) Rose, A. In *Concepts in photoconductivity and allied problems*; Interscience: New York, 1963. (b) Meier, H. In *Organic Semiconductors*; Verlag Chemie: Berlin, 1974.

excess electrons to the substrate is not large enough, they will accumulate in the film and neutralize with holes, decreasing therefore the total collected photocurrent. In that case, back-side illumination will result in larger quantum efficiencies than will front-side illumination.

On the contrary, for nonporous films the interface between the film and the solution is limited to the film surface. Front illumination would therefore generate more excess holes and electrons near the active interface than back illumination for which a filtering effect is expected if the exciton diffusion length is less than the film thickness. A larger quantum yield is then expected for front illumination of a nonporous film.

The filtering effect is well illustrated in Figure 5B compared to Figure 5A for compound 2. It is not seen for a film thickness of 300 Å, but it i well observed for a 1750-Å-thick film. Exciton diffusion length in material 2 is therefore comprised between 330 and 1750 Å. As far as Figure 6 is concerned, both directions of illumination give nearly identical action spectra for porous films of compound 6. Some filtering effect appears for front illumination for thickner films but is much less effective than the back illumination of compound 2, although both materials are characterized by a similar thickness absorption spectrum and maximum absorption coefficient. Some filtering effect is expected for the front illumination of a porous film of high-resistance material because lower photocurrent would be collected from the nonsubstrate region than from the near substrate region of the film. The active interface is however always the film–solution interface and not the film–SnO_2 interface. Lowering the resistance of a porous film by increasing the charge carrier density or mobility or the kinetics of charge transfer between crystallites would result in the disappearance of the filtering effect for front illumination, and thus front and back illuminations would yield the same action spectrum regardless of the thickness of the film. This was indeed observed for PTCDA.[9]

Conclusion

The present work about the photoelectrochemical properties of some perylene derivatives has been undertaken to find out the best material to use in heterojunctions with chloroaluminum phthalocyanine, a p-type molecular semiconductor already studied extensively in our group. All perylenes investigated show a dominant photoanodic behavior. However, they need not be n-type semiconductors. Among all perylene derivatives studied, material 2 is by far the most photoactive. It also forms compact nonporous films at the substrate temperature of 160 °C and the growth rate of 0.8 Å s^{-1} used. The nonporous character of material 2 films is important because the highly photoactive chloroaluminum phthalocyanine films grown at 2000 Å s^{-1} are porous, and the junction of two porous films could lead to short circuits between the two collecting electrodes.

Registry No. 1, 128-65-4; 2, 6424-77-7; 3, 22047-48-9; 4, 2379-77-3; 5, 67075-37-0; 6, 136847-29-5; 7 (cis isomer), 55034-81-6; 7 (trans isomer), 55034-79-2; SnO_2, 18282-10-5; chloroaluminum phthalocyanine, 14154-42-8; 3,4,9,10-perylenetetracarboxylic dianhydride, 128-69-8; aniline, 62-53-3; *p*-anisidine, 104-94-9; 2,4-dimethylaniline, 95-68-1; 4-chloroaniline, 106-47-8; phenethylamine, 64-04-0; 4-aminopyridine, 504-24-5; 1,2-phenylenediamine, 95-54-5; KHP, 877-24-7; H_2Q, 123-31-9; $Fe(CN)_6^{3-}$, 13408-62-3; $Fe(CN)_6^{4-}$, 13408-63-4; I_3^-, 14900-04-0; I^-, 20461-54-5; benzoquinone, 106-51-4.

Volatile Barium β-Diketonate Polyether Adducts. Synthesis, Characterization, and Metalloorganic Chemical Vapor Deposition

R. Gardiner,* D. W. Brown,* and P. S. Kirlin*

Advanced Technology Materials, Inc., 7 Commerce Drive, Danbury, Connecticut 06810

A. L. Rheingold

Department of Chemistry, University of Delaware, Newark, Delaware 19716

Received May 1, 1991. Revised Manuscript Received August 26, 1991

The 2,5,8,11,14-pentaoxopentadecane (tetraglyme) adducts of barium complexes of 1,1,1,5,5,5-hexafluoro-2,4-pentanedione (H(hfacac)), 1,1,1-trifluoro-2,4-pentanedione (H[tfacac]), and 2,2,6,6-tetramethyl-3,5-heptanedione (H(thd)) have been prepared and characterized by X-ray crystallography, ^1H and ^{13}C NMR spectroscopies, melting and sublimation points, and elemental analysis. The thermal stability of the complexes is related to their solid-state structure in which the coordination number around the barium atom is nine with a monocapped, twisted square prism structure. Metalloorganic chemical vapor deposition experiments were performed using the 1,1,1,5,5,5-hexafluoro-2,4-pentanedionato and 1,1,1-trifluoro-2,4-pentanedionato complexes; the 2,2,6,6-tetramethyl-3,5-heptanedionato complex dissociated prior to sublimation. The as-deposited barium fluoride films were characterized by scanning electron microscopy and energy-dispersive X-ray spectroscopy.

Introduction

Since the discovery of superconductivity above 30 K in 1986,[1] numerous research efforts have focused on thin-film preparation of these materials for microelectronic applications. Metalloorganic chemical vapor deposition (MOCVD) has significant advantages relative to physical vapor deposition (PVD) methods in the growth of superconducting thin films; large wafers can be uniformly coated, and scale up to large volumes is easily accom-

(1) Bednorz, J. G.; Muller, K. A. *Z. Phys. B* **1986**, *64*, 189.

0897-4756/91/2803-1053$02.50/0